Probing New Physics in Dimension-8 Neutral Gauge Couplings at e^+e^- Colliders

Rui-Qing Xiao

Shanghai Jiao Tong University

J. Ellis, H. J. He and R. Q. Xiao, Science China (Phys. Mech. Astron.) 64 (2021) 221062 [arXiv:2008.04298 [hep-ph]]

J. Ellis, S. F. Ge, H. J. He, and R. Q. Xiao, Chin. Phys. C 44 (2020) 063106, no. 6 [arXiv:1902.06631 [hep-ph]]

CP-conserving effective operators for neutral triple gauge couplings (nTGCs)

nTGCs are absent in tree level SM and SMEFT up to Dimension-6
Dimension-8 can contribute to the nTGCs

$$\Delta\mathcal{L}(\text{dim-8}) = \sum_{j=1}^{4} \frac{c_j}{\tilde{\Lambda}^4}\mathcal{O}_j = \sum_{j=1}^{4} \frac{\text{sign}(c_j)}{\Lambda_j^4}\mathcal{O}_j \,,$$

Operators with Higgs field:

$$\begin{aligned}
\mathcal{O}_{\widetilde{B}W} &= \mathrm{i}\, H^\dagger \widetilde{B}_{\mu\nu} W^{\mu\rho}\{D_\rho, D^\nu\}H + \text{h.c.},\\
\mathcal{O}_{B\widetilde{W}} &= \mathrm{i}\, H^\dagger B_{\mu\nu} \widetilde{W}^{\mu\rho}\{D_\rho, D^\nu\}H + \text{h.c.},\\
\mathcal{O}_{\widetilde{W}W} &= \mathrm{i}\, H^\dagger \widetilde{W}_{\mu\nu} W^{\mu\rho}\{D_\rho, D^\nu\}H + \text{h.c.},
\end{aligned}$$

$$\mathcal{O}_{\widetilde{B}B} = \mathrm{i}\, H^\dagger \widetilde{B}_{\mu\nu} B^{\mu\rho}\{D_\rho, D^\nu\}H + \text{h.c.},$$

$\mathcal{O}_{B\widetilde{W}}$ is equivalent to $\mathcal{O}_{\widetilde{B}W}$
$\mathcal{O}_{\widetilde{W}W}$ and $\mathcal{O}_{\widetilde{B}B}$ do not contribute to $ZV\gamma$ coupling for on-shell Z and γ.

Pure Gauge operators:

$$\begin{aligned}
g\mathcal{O}_{G+} &= \widetilde{B}_{\mu\nu} W^{a\mu\rho}(D_\rho D_\lambda W^{a\nu\lambda} + D^\nu D^\lambda W^a_{\lambda\rho}),\\
g\mathcal{O}_{G-} &= \widetilde{B}_{\mu\nu} W^{a\mu\rho}(D_\rho D_\lambda W^{a\nu\lambda} - D^\nu D^\lambda W^a_{\lambda\rho}).
\end{aligned}$$

Using the equation of motion, both of these operators can be related to a sum of operators with additional Higgs doublets and additional fermion bilinears:

$$\begin{aligned}
\mathcal{O}_{G+} &= \{\mathrm{i}H^\dagger \widetilde{B}_{\mu\nu} W^{\mu\rho}[D_\rho, D^\nu]H + \mathrm{i}\,2(D_\rho H)^\dagger \widetilde{B}_{\mu\nu} W^{\mu\rho} D^\nu H + \text{h.c.}\} + \mathcal{O}_{C-}\,,\\
\mathcal{O}_{G-} &= \mathcal{O}_{\widetilde{B}W} + \mathcal{O}_{C+}\,,
\end{aligned}$$

where $\mathcal{O}_{C+}$ and $\mathcal{O}_{C-}$ denote the following dimension-8 fermionic contact operators:

$$\begin{aligned}
\mathcal{O}_{C+} &= \widetilde{B}_{\mu\nu} W^{a\mu\rho}\left[D_\rho(\overline{\psi_L} T^a \gamma^\nu \psi_L) + D^\nu(\overline{\psi_L} T^a \gamma_\rho \psi_L)\right],\\
\mathcal{O}_{C-} &= \widetilde{B}_{\mu\nu} W^{a\mu\rho}\left[D_\rho(\overline{\psi_L} T^a \gamma^\nu \psi_L) - D^\nu(\overline{\psi_L} T^a \gamma_\rho \psi_L)\right].
\end{aligned}$$

NTGC Vertex

$\mathcal{O}_{G+}$ contributes to both the $Z\gamma Z^*$ and $Z\gamma\gamma^*$ vertices in the following forms:

$$\Gamma^{\alpha\beta\mu}_{Z\gamma Z^*+}(q_1, q_2, q_3) \;=\; -\mathrm{sign}(\tilde{c}_{G+})\frac{v(q_3^2 - M_Z^2)}{M_Z\Lambda^4}\left(q_3^2\, q_{2\nu}\epsilon^{\alpha\beta\mu\nu} + 2q_2^\alpha\, q_{3\nu}\, q_{2\sigma}\epsilon^{\beta\mu\nu\sigma}\right),$$

$$\Gamma^{\alpha\beta\mu}_{Z\gamma\gamma^*+}(q_1, q_2, q_3) \;=\; -\mathrm{sign}(\tilde{c}_{G+})\frac{s_W v\, q_3^2}{c_W M_Z\Lambda^4}\left(q_3^2\, q_{2\nu}\epsilon^{\alpha\beta\mu\nu} + 2q_2^\alpha\, q_{3\nu}\, q_{2\sigma}\epsilon^{\beta\mu\nu\sigma}\right),$$

Contributions from the initial-state right-handed fermions to the sum of the amplitudes $\mathcal{T}[f\bar{f}\to Z^*\to Z\gamma]$ and $\mathcal{T}[f\bar{f}\to\gamma^*\to Z\gamma]$ vanish.
$\mathcal{O}_{G-}$ contribution to the nTGC coupling $Z\gamma\gamma^*$,

$$\mathrm{i}\,\Gamma^{\alpha\beta\mu}_{Z\gamma\gamma^*-}(q_1, q_2, q_3) \;=\; -\mathrm{sign}(\tilde{c}_-)\frac{s_W vM_Z}{c_W\Lambda^4}\epsilon^{\alpha\beta\mu\nu}q_{2\nu}q_3^2\,,$$

for on-shell gauge bosons Z and γ plus a virtual photon γ^*.

Higgs-related dimension-8 operator $\mathcal{O}_{\widetilde{B}W}$ yields the following effective $Z\gamma Z^*$ coupling,

$$\mathrm{i}\,\Gamma^{\alpha\beta\mu}_{Z\gamma Z^*(\widetilde{B}W)}(q_1, q_2, q_3) \;=\; \mathrm{sign}(\tilde{c}_{\widetilde{B}W})\frac{vM_Z(q_3^2 - M_Z^2)}{\Lambda^4}\epsilon^{\alpha\beta\mu\nu}q_{2\nu}\,.$$

$Z\gamma$ Production at e^+e^- Colliders

Kinematical structure of the reaction $e^+(p_1)e^-(p_2) \to Z(q_1)\gamma(q_2) \to \gamma(q_2)f(k_1)\bar{f}(k_2)$

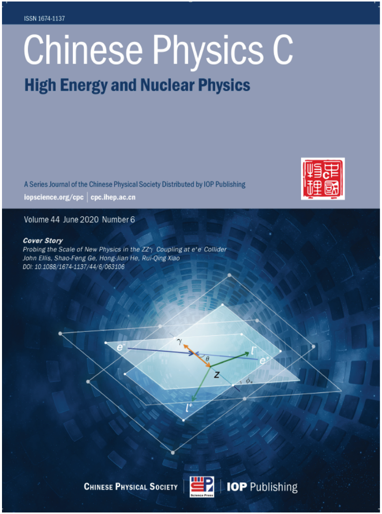

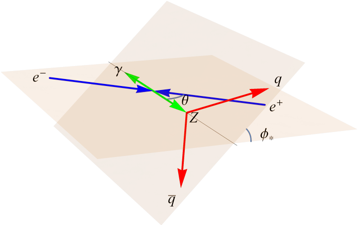

$$
\begin{aligned}
p_1 &= E_1(1,0,0,1), \;\; p_2 = E_1(1,0,0,-1),\\
q_1 &= (E_Z,\; q\sin\theta,\; 0,\; q\cos\theta),\\
q_2 &= q(1,\; -\sin\theta,\; 0,\; -\cos\theta),
\end{aligned}
$$

$$
E_1 = \frac{\sqrt{s}}{2}\,,\; q = \frac{s-M_Z^2}{2\sqrt{s}}\,,\; E_Z = \sqrt{q^2+M_Z^2}\,.
$$

$$
k_1 = \frac{M_Z}{2}\,(1,\; \sin\theta_*\cos\phi_*,\; \sin\theta_*\sin\phi_*,\; \cos\theta_*)\,,
$$

$$
k_2 = \frac{M_Z}{2}\,(1,\; -\sin\theta_*\cos\phi_*,\; -\sin\theta_*\sin\phi_*,\; -\cos\theta_*)\,.
$$

Feynman Diagrams

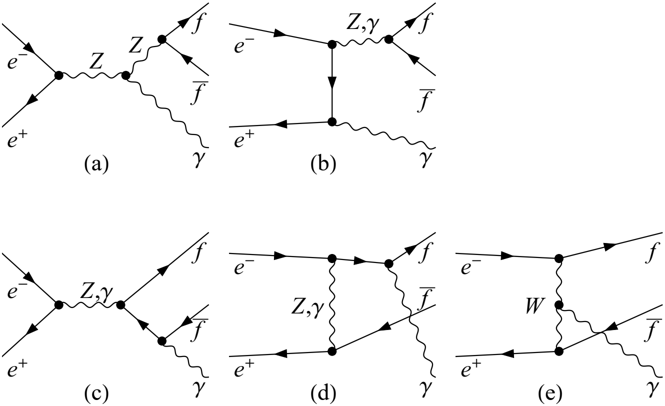

Signal: (a);
Irreducible background: (b) (with on-shell Z);
Reducible background: other diagrams.
For analytical study, we only consider (a) and (b). All diagrams are included in numerical results.

Total cross section for $e^+e^- \to Z\gamma$, including the contributions of $\mathcal{O}_{G+}$:

$$\sigma_+(Z\gamma) = \frac{e^4(c_L^2+c_R^2)\left[-(s-M_Z^2)^2-2(s^2+M_Z^4)\ln\sin\frac{\delta}{2}\right]}{8\pi s_W^2 c_W^2 (s-M_Z^2)s^2} + \mathrm{sign}(\tilde{c}_{G+})\frac{e^2 c_L x_L M_Z^2(s-M_Z^2)}{4\pi s_W c_W\, s}\frac{1}{\Lambda^4} + \frac{x_L^2(s+M_Z^2)(s-M_Z^2)^3}{48\pi\, s}\frac{1}{\Lambda^8} + O(\delta)\,,$$

Define $f_\xi^j = \frac{\mathrm{d}\sigma_j}{\sigma_j \mathrm{d}\xi}$

where the angles $\xi \in (\theta,\ \theta_*,\ \phi_*)$, and the cross sections σ_j $(j=0,1,2)$ represent the SM contribution (σ_0), the $\mathcal{O}(\Lambda^{-4})$ contribution (σ_1), and the $\mathcal{O}(\Lambda^{-8})$ contribution (σ_2), respectively.

$f_{\phi_*}^j$ for quarks:

$$f_{\phi_*}^0 = \frac{1}{2\pi} + \frac{3\pi^2(c_L^2-c_R^2)^2 M_Z\sqrt{s}\,(s+M_Z^2)\cos\phi_* - 8(c_L^2+c_R^2)^2 M_Z^2\, s\cos 2\phi_*}{16\pi(c_L^2+c_R^2)^2\left[(s-M_Z^2)^2+2(s^2+M_Z^4)\ln\sin\frac{\delta}{2}\right]} + O(\delta),$$

$$f_{\phi_*+}^1 = \frac{1}{2\pi} - \frac{3\pi(q_L^2-q_R^2)(M_Z^2+5s)\cos\phi_*}{256(q_L^2+q_R^2)M_Z\sqrt{s}} + \frac{s\cos 2\phi_*}{8\pi M_Z^2},$$

$$f_{\phi_*+}^2 = \frac{1}{2\pi} - \frac{9\pi(q_L^2-q_R^2)M_Z\sqrt{s}\cos\phi_*}{128(q_L^2+q_R^2)(s+M_Z^2)},$$

The coefficients $(c_L,\ c_R) = (-\frac{1}{2}+s_W^2,\ s_W^2)$ and $(q_L,\ q_R) = (T_3 - Q s_W^2,\ -Q s_W^2)$.

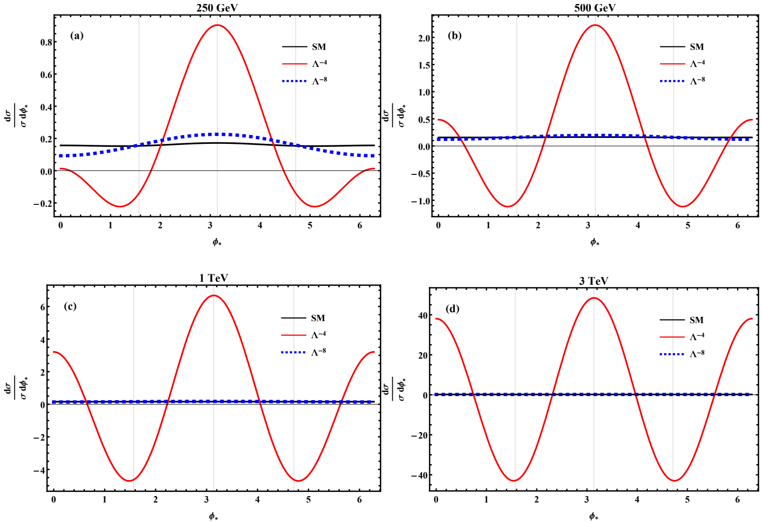

Normalized angular distributions in the azimuthal angle ϕ_* for $e^- e^+ \to Z\gamma$ followed by $Z \to d\bar{d}$ decays, as generated by $\mathcal{O}_{G+}$ at the collision energies $\sqrt{s} = (0.25,\ 0.5,\ 1,\ 3)$ TeV, respectively. In each plot, the black, red, and blue curves denote the contributions from the SM, the interference term of $\mathcal{O}(\Lambda^{-4})$, and the quadratic term of $\mathcal{O}(\Lambda^{-8})$, respectively, where we note that the blue and black curves almost coincide. We have imposed a basic cut on the polar scattering angle, $\sin\theta > \sin\delta$, with $\delta = 0.2$ for illustration.

$\mathcal{O}_{G-}$, $\mathcal{O}_{\widetilde{B}W}$ and $\mathcal{O}_{C+}$:

$$
\begin{aligned}
\sigma(Z\gamma) \;=\;& \frac{e^4(c_L^2+c_R^2)\big[-(s-M_Z^2)^2-2(s^2+M_Z^4)\ln\sin\frac{\delta}{2}\,\big]}{8\pi s_W^2 c_W^2 (s-M_Z^2)s^2} \\
&+\mathrm{sign}(\tilde{c}_j)\,\frac{e^2(c_L x_L-c_R x_R)M_Z^2\,(s-M_Z^2)\,(s+M_Z^2)}{8\pi s_W c_W\, s^2}\,\frac{1}{\Lambda^4} \\
&+\frac{(x_L^2+x_R^2)M_Z^2\,(s+M_Z^2)\,(s-M_Z^2)^3}{48\pi\, s^2}\,\frac{1}{\Lambda^8}\;+\,O(\delta)\,,
\end{aligned}
$$

where the relevant coupling coefficients $(x_L,\, x_R)$ are defined as

$$
\begin{aligned}
(x_L,\, x_R) \;&=\; (s_W^2,\, s_W^2), && (\text{for } \mathcal{O}_j=\mathcal{O}_{G-}), \\
(x_L,\, x_R) \;&=\; \left(-\tfrac{1}{2}+s_W^2,\, s_W^2\right), && (\text{for } \mathcal{O}_j=\mathcal{O}_{\widetilde{B}W}), \\
(x_L,\, x_R) \;&=\; (\tfrac{1}{2},\, 0), && (\text{for } \mathcal{O}_j=\mathcal{O}_{C+}).
\end{aligned}
$$

The normalized angular distribution functions $f^j_{\phi*}$ for quarks,

$$
\begin{aligned}
f^0_{\phi*} \;&=\; \frac{1}{2\pi}+\frac{3\pi^2 c_-^2\, q_-^2\, M_Z\sqrt{s}\,(s+M_Z^2)\cos\phi_* - 8c_+^2 q_+^2 M_Z^2\, s\cos 2\phi_*}{16\pi c_{LR+}^2 q_+^2\left[(s-M_Z^2)^2+2(s^2+M_Z^4)\ln\sin\frac{\delta}{2}\right]}+O(\delta), \\
f^1_{\phi*} \;&=\; \frac{1}{2\pi}-\frac{9\pi(c_L x_L+c_R x_R)(q_L^2-q_R^2)\sqrt{s}\,\cos\phi_*}{128(c_L x_L-c_R x_R)(q_L^2+q_R^2)M_Z}+\frac{s\cos 2\phi_*}{4\pi(s+M_Z^2)}\,, \\
f^2_{\phi*} \;&=\; \frac{1}{2\pi}-\frac{9\pi(x_L^2-x_R^2)(q_L^2-q_R^2)M_Z\sqrt{s}\,\cos\phi_*}{128(x_L^2+x_R^2)(q_L^2+q_R^2)(s+M_Z^2)}\,,
\end{aligned}
$$

with the coefficients $(c_\pm^2,\, q_\pm^2)=(c_L^2\pm c_R^2,\, q_L^2\pm q_R^2)$.

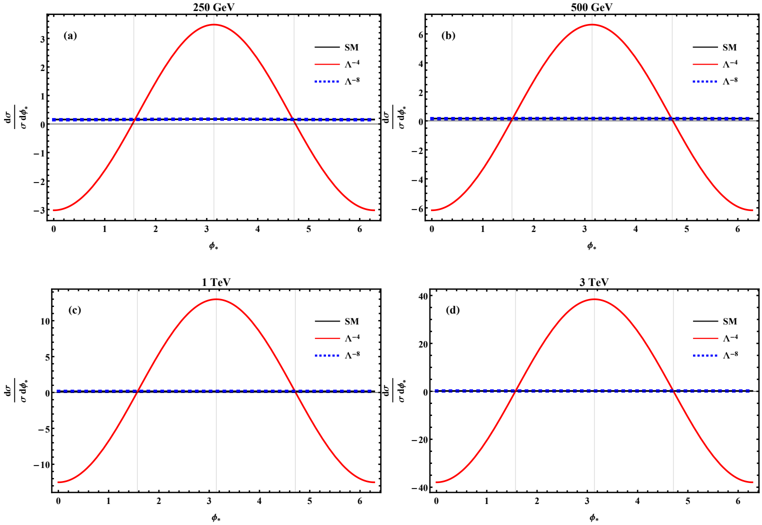

Normalized angular distributions in the azimuthal angle ϕ_* for $e^- e^+ \to Z\gamma$ followed by $Z \to d\bar{d}$ decays, as generated by $\mathcal{O}_{\widetilde{B}W}$ at the collision energies $\sqrt{s} = (0.25,\ 0.5,\ 1,\ 3)$ TeV, respectively. In each plot, the black, red, and blue curves denote the contributions from the SM, the interference term of $O(\Lambda^{-4})$, and the quadratic term of $O(\Lambda^{-8})$, respectively, where we note that the blue and black curves almost coincide. We have imposed a basic cut on the polar scattering angle, $\sin\theta > \sin\delta$, with $\delta = 0.2$ for illustration.

For $\mathcal{O}_{G+}$, we note that the $\cos 2\phi_*$ term dominates $f^1_{\phi_*}$. Thus, we can construct the following observable $\mathbb{O}^c_1$:

$$\mathbb{O}^c_1 \quad \equiv \quad \left|\sigma_1 \int \mathrm{d}\theta \mathrm{d}\theta_* \mathrm{d}\phi_* \mathrm{d}M_* \, f_j^{(4)} \mathrm{sign}(\cos 2\phi_*)\right|,$$

where

$$f_j^{(4)} \; = \; \frac{\mathrm{d}^4\sigma_j}{\sigma_j \, \mathrm{d}\theta \, \mathrm{d}\theta_* \mathrm{d}\phi_* \mathrm{d}M_*} \, .$$

For $\mathcal{O}_{G-}$, $\mathcal{O}_{\widetilde{B}W}$ and $\mathcal{O}_{C+}$, the leading term in the differential cross section at $O(\Lambda^{-4})$ is proportional to

$$\frac{v^2\sqrt{s}}{\Lambda^4 M_Z}\left[C_1(1+\cos^2\theta) + C_2 \cos\theta \cos\theta_*\right] \sin^2\theta_* \cos\phi_* \, ,$$

where the coefficients $C_1 = (c_L x_L + c_R x_R)(q_L^2 - q_R^2)$ and $C_2 = 2(c_L x_L - c_R x_R)(q_L^2 + q_R^2)$. We construct the following observable $\mathbb{O}^c_1$ for the effective operator $\mathcal{O}_{G-}$:

$$\mathbb{O}^c_1 \; = \; \left|\sigma_1 \int \mathrm{d}\theta \mathrm{d}\theta_* \mathrm{d}\phi_* \mathrm{d}M_* \, f_1^{(4)} \mathrm{sign}(\cos\theta) \, \mathrm{sign}(\cos\theta_*) \, \mathrm{sign}(\cos\phi_*)\right|.$$

And $\mathbb{O}^c_1$ for the effective operator $\mathcal{O}_{\tilde{B}W}$:

$$\mathbb{O}^c_1 \; = \; \left|\sigma_1 \int \mathrm{d}\theta \mathrm{d}\theta_* \mathrm{d}\phi_* \mathrm{d}M_* \, f_1^{(4)} \mathrm{sign}(\cos\phi_*)\right|.$$

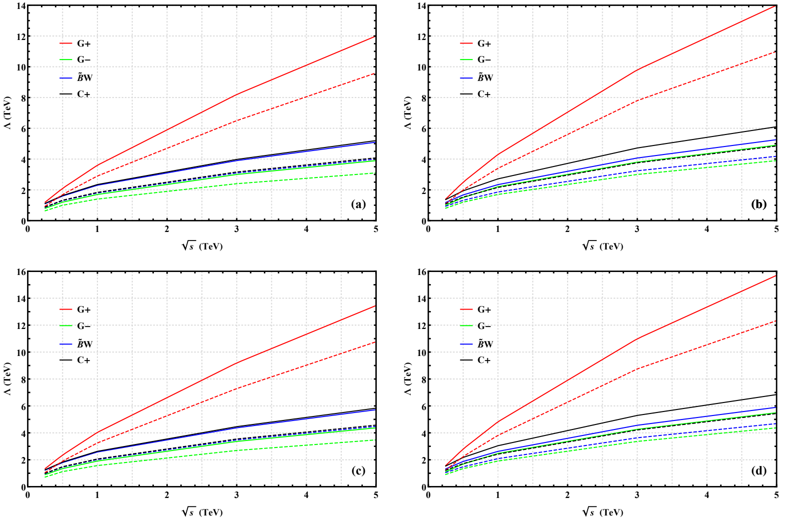

Reaches of the new physics scale Λ as functions of the e^+e^- collision energy $\sqrt{s}$. In each plot, the combined sensitivities are presented at 2σ (solid curve) and 5σ (dashed curve) levels, and for each individual dimension-8 operator among $(\mathcal{O}_{G+},\ \mathcal{O}_{G-},\ \mathcal{O}_{\widetilde{B}W},\ \mathcal{O}_{C+})$ which correspond to the (red, purple, blue, black) curves, respectively. Plots (a) and (c) are for unpolarized $e^{\mp}$ beams, whereas plots (b) and (d) are for polarized $e^{\mp}$ beams with $(P_L^e,\ P_R^{\bar{e}}) = (0.9,\ 0.65)$. The plots (a) and (b) have input a sample integrated luminosity $\mathcal{L} = 2\,\mathrm{ab}^{-1}$, while the plots (c) and (d) have used as input a sample of $\mathcal{L} = 5\,\mathrm{ab}^{-1}$.

$\sqrt{s}$	$\Lambda^{2\sigma}_{G+}$	$\Lambda^{5\sigma}_{G+}$	$\Lambda^{2\sigma}_{G-}$	$\Lambda^{5\sigma}_{G-}$	$\Lambda^{2\sigma}_{\widetilde{B}W}$	$\Lambda^{5\sigma}_{\widetilde{B}W}$	$\Lambda^{2\sigma}_{C+}$	$\Lambda^{5\sigma}_{C+}$
0.25	(1.3, 1.6)	(1.0, 1.2)	(0.9, 1.1)	(0.72, 0.89)	(1.2, 1.3)	(0.97, 1.0)	(1.2, 1.6)	(0.97, 1.2)
0.5	(2.3, 2.7)	(1.9, 2.2)	(1.3, 1.7)	(1.1, 1.3)	(1.8, 1.9)	(1.4, 1.4)	(1.8, 2.2)	(1.4, 1.7)
1	(3.9, 4.7)	(3.2, 3.7)	(1.9, 2.4)	(1.6, 1.9)	(2.6, 2.6)	(2.0, 2.1)	(2.6, 2.9)	(2.0, 2.4)
3	(9.2, 11.0)	(7.2, 8.6)	(3.3, 4.2)	(2.7, 3.3)	(4.3, 4.5)	(3.5, 3.6)	(4.4, 5.2)	(3.4, 4.1)
5	(13.4, 15.9)	(10.8, 12.7)	(4.4, 5.5)	(3.4, 4.4)	(5.7, 5.9)	(4.5, 4.7)	(5.7, 6.8)	(4.5, 5.5)

Sensitivity reaches of the new physics scale Λ (in TeV) for each of the dimension-8 nTGC operators or related contact operator ($\mathcal{O}_{G+}$, $\mathcal{O}_{G-}$, $\mathcal{O}_{\widetilde{B}W}$, $\mathcal{O}_{C+}$), at the 2σ (exclusion) and 5σ (discovery) levels, as obtainable from the reaction $e^-e^+ \to Z\gamma \to q\bar{q}\gamma$ at different collider energies $\sqrt{s}$ (in TeV), with (unpolarized, polarized) $e^\mp$ beams as marked by (blue, red) colors in each entry. We choose a sample integrated luminosity $\mathcal{L} = 5\,\text{ab}^{-1}$ and the $e^\mp$ beam polarizations $(P^e_L,\ P^{\bar{e}}_R) = (0.9,\ 0.65)$.

$\sqrt{s}$ (energy)	$\mathcal{L}$ (ab^{-1})	$\Lambda_{G+}^{\ell,2\sigma}$ (unpol, pol)	$\Lambda_{G+}^{\ell,5\sigma}$ (unpol, pol)	$\Lambda_{\widetilde{B}W}^{\ell,2\sigma}$ (unpol, pol)	$\Lambda_{\widetilde{B}W}^{\ell,5\sigma}$ (unpol, pol)
250 GeV	2	(0.93, 1.1)	(0.74, 0.87)	(0.56, 0.65)	(0.44, 0.51)
	5	(1.0, 1.2)	(0.83, 0.97)	(0.63, 0.73)	(0.49, 0.57)
500 GeV	2	(1.7, 2.0)	(1.3, 1.5)	(0.8, 1.0)	(0.64, 0.78)
	5	(1.9, 2.2)	(1.4, 1.7)	(0.90, 1.1)	(0.72, 0.87)
1 TeV	2	(2.8, 3.3)	(2.3, 2.7)	(1.2, 1.4)	(0.91, 1.1)
	5	(3.1, 3.7)	(2.6, 3.0)	(1.3, 1.6)	(1.0, 1.2)
3 TeV	2	(6.5, 7.7)	(5.1, 6.0)	(2.0, 2.5)	(1.6, 2.0)
	5	(7.3, 8.6)	(5.7, 6.7)	(2.2, 2.8)	(1.8, 2.2)
5 TeV	2	(9.5, 11.2)	(7.5, 8.8)	(2.6, 3.2)	(2.0, 2.6)
	5	(10.6, 12.5)	(8.4, 9.9)	(2.9, 3.6)	(2.2, 2.9)

Sensitivities for probes of the new physics scale Λ (in TeV) of the nTGC pure gauge operator $\mathcal{O}_{G+}$ in comparison with that of the Higgs-related nTGC operator $\mathcal{O}_{\widetilde{B}W}$, at the 2σ (exclusion) and 5σ (discovery) levels for different dimension-8 operators, as obtained from the reaction $e^-e^+\!\to Z\gamma\to\ell\bar{\ell}\gamma$ at different collider energies, for $\mathcal{L}=2\,\text{ab}^{-1}$ and $\mathcal{L}=5\,\text{ab}^{-1}$, respectively. The sensitivity limits on Λ are shown in pair inside the parentheses of each entry and correspond to the cases with (unpolarized, polarized) $e^\mp$ beams, which are marked with (blue, red) colors and under the abbreviations (unpol, pol) in the second row. The polarized $e^\mp$ beams correspond to $(P_L^e,\ P_R^{\bar{e}})=(0.9,\ 0.65)$.

Conculsion

- We study systematically how dimension-8 operators that contribute to neutral triple gauge couplings (nTGCs) can be probed via the reaction $e^+e^- \to Z\gamma$
- We have constructed a new set of dimension-8 CP-conserving pure gauge operators $\mathcal{O}_{G+}$ that contribute to the nTGC vertices with a leading energy dependence $\propto E^5$.
- Hadronic Z decays with larger branching fractions increases the sensitivity significantly, as compared to leptonic decay channels.
- Dimension-8 pure gauge operator $\mathcal{O}_{G+}$ provides the most sensitive probe to the new physics scale of nTGCs, namely, the Λ_{G+} can be probed up to the range $(1-5)$ TeV for the CEPC, FCC-ee and ILC colliders with $\sqrt{s}=(0.25-1)$ TeV, and up to the range $(10-16)$ TeV for CLIC with $\sqrt{s}=(3-5)$ TeV, choosing in each case a sample integrated luminosity of $\mathcal{L}=5\,\text{ab}^{-1}$.
- The present findings demonstrate that the reaction $e^+e^- \to Z\gamma$ provides an important opportunity to explore the dimension-8 SMEFT contributions to nTGCs, with sensitivity reaches of the corresponding new physics scales extending well into the multi-TeV range.

Thank you!